CHAPTER IV
RESULTS AND DISCUSSION

4.1 The Microscopic and Macroscopic Stability of the Oil-in-Water Emulsion

Microscopic and macroscopic stability of the prepared emulsions were characterized prior to statistical analysis of dispersed oil, regarding the volume-based mean diameter (VMD) and droplet size distribution (DSD).

In order to observe the dispersion of oil in water, the water soluble dye – Methylene blue trihydrate, was used to distinguish the dispersed oil phase from the water continuous phase and also to identify the appearance of oil in absence of surfactant, oil-in-water emulsion with oil fraction at 50 vol% and oil-in-water mixture were prepared as shown in Figure 4.1.

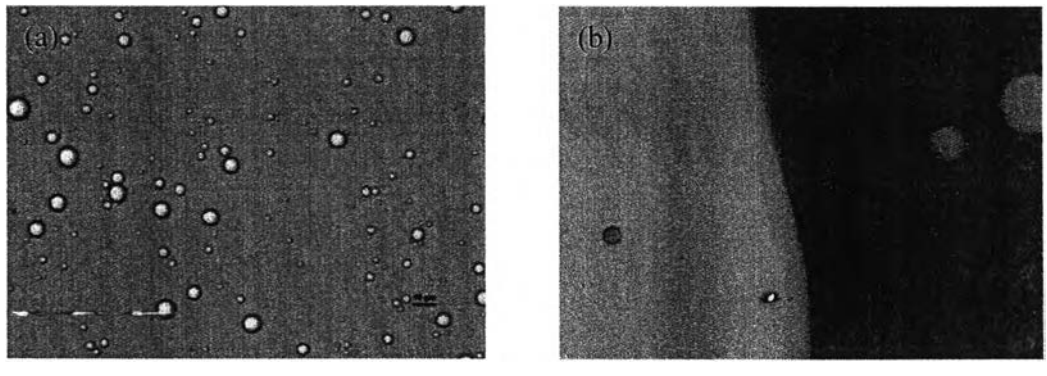

Figure 4.1 (a) Oil fully dispersed as colorless droplets in blue water continuous phase (diluted 10 times), (b) Oil-in-water mixture completely separated and formed an interface between both phases.

Figure 4.1(a) shows that oil droplets (colorless) were fully dispersed in the water continuous phase (blue) with visually well-dispersed droplets. Notice that the original emulsion was diluted 10 times prior to characterization of microscopic stability. Comparing with the oil-in-water dispersion in presence of surfactant, oil and water phases completely separated as shown in Figure 4.1(b). Further microscopic and macroscopic stability of prepared emulsion was evaluated.

Prior to the microstructure characterization of oil-in-water emulsion, macroscopic stability of oil-in-water emulsion was investigated throughout a period of 48 hours by observing the variation of separated water volume. The emulsion appearances were photographed immediately after the emulsion preparation and after 48 hours. The emulsion initially appeared milky as is shown in Figure 4.2. A clear water phase appeared at the bottom of a vial as time proceeded and eventually separated into two different phases of a milky top phase, similar to the initial emulsion appearance and a clear bottom phase presumed to be a separated water phase.

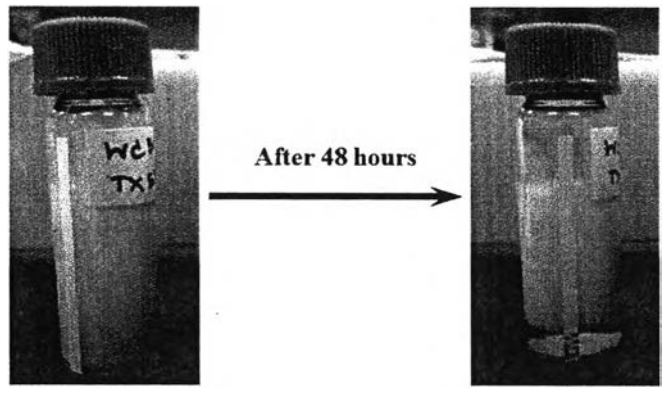

Figure 4.2 Phase separation was observed throughout a period of 48 hours for oil fraction at 50 vol%.

Macroscopic stability observation indicated rapid phase separation of oil-in-water emulsion for low oil fraction and slower phase separation with increasing of oil fraction as shown in Figure 4.3. Approximately 80 vol% of water settled to the bottom of the vial as a separated phase in 5 minutes for oil fraction at 10 vol% while the phase separation reached plateau around 45 vol% after 24 hours as oil fraction was increased to 50 vol%. Variation of separated water volume showed macroscopic instability of oil-in-water emulsion.

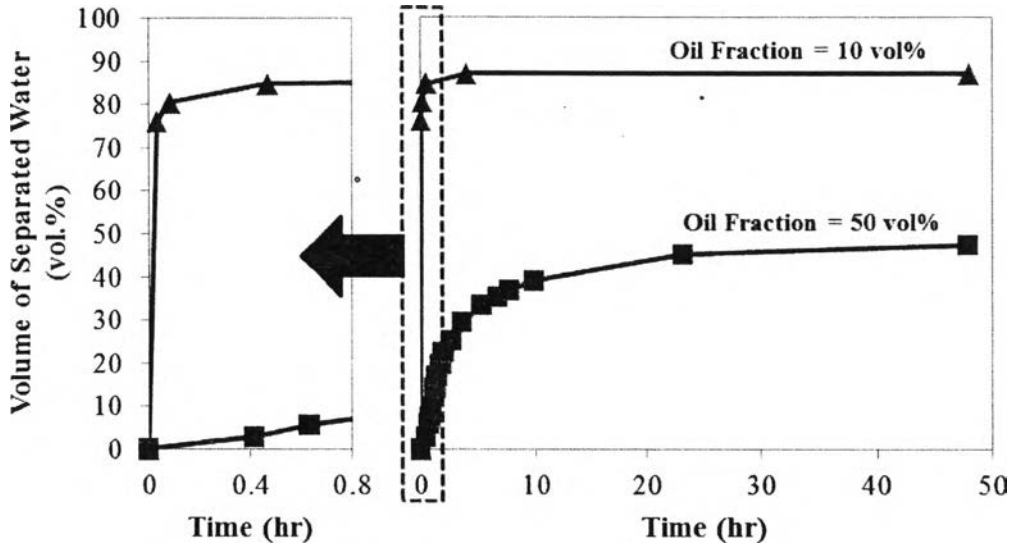

Figure 4.3 Variation of volume of separated water as a function of time for oil fraction at 10 vol% and 50 vol%.

Similar phase separation was also observed by Egger and McGrath (2006) where they conducted oil-in-water emulsion using n-Octane aiding with Triton X-100 by Triton X-100 to oil ratio of 1:5. They found an increasingly change in size of droplets as 0.45 μm grew to 11 μm after 336 hours. Also, the mechanism of their oil-in-water emulsion was evaluated by fitting the droplet size with different correlations including standard Ostwald ripening, enhanced Ostwald ripening, and coalescence. They believed that the destabilization mechanism of their emulsion consisted of two mechanisms: the enhanced Ostwald ripening mechanism played a role initially, then followed by standard Ostwald ripening or creaming mechanism. Obtaining the Ostwald ripening rate required several microstructure analyses. Nevertheless, the phase separation mechanism could be characterized with lesser data points and time.

To identify the phase separation mechanism of prepared oil-in-water emulsion, microstructure evolution was characterized with microscope. Emulsion was sampled twice, immediately after emulsion preparation and after 48 hours. As shown in the microscopic observation, the second sampling was conducted with both oil-in-water emulsion phase (upper phase) and separated water phase (lower phase)

for resolving the phase separation mechanism. The first sample, so called *initial emulsion*, indicated well dispersed oil droplets in water continuous phase while the second sampling indicated concentrated oil droplets in the upper phase, termed as *oil-rich phase*. The oil-rich phase revealed visually similar distribution and size of oil droplets, but few oil droplets were observed in separated water phase or lower phase. Based on microstructure characterization, oil droplets remained dispersed in oil-rich phase after phase separation as shown in Figure 4.4. Therefore, the phase separation of oil-in-water dispersion underwent gravitational settling mechanism where there was no significant coalesce observed over 48 hours.

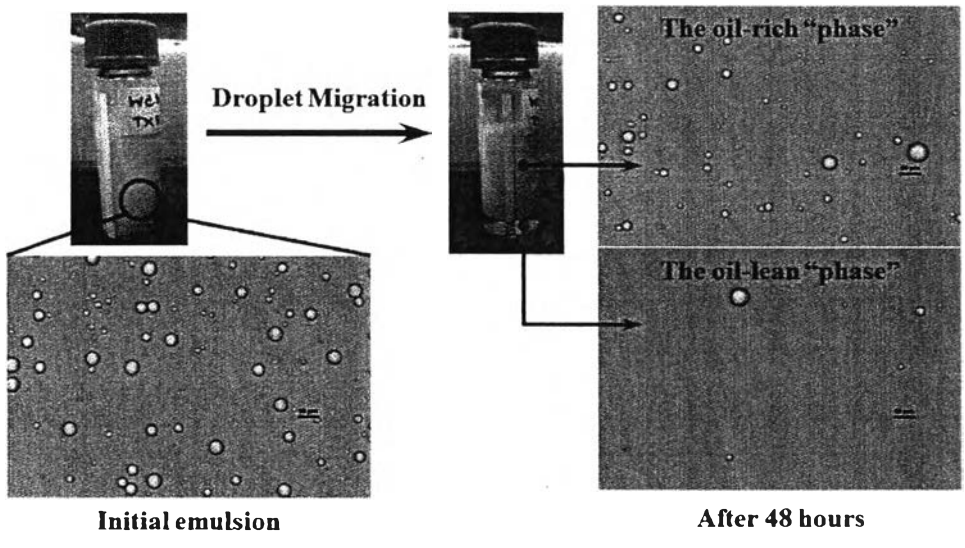

Figure 4.4 The microstructure of oil-in-water emulsion for initial emulsion and both an oil-rich phase and an oil-lean phase after phase separation for oil fraction at 50 vol%.

Addition to the microstructure characterization, quantitative analysis of the VMD and the DSD of dispersed oil were evaluated. The VMD indicated insignificant change over 48 hours for both oil fraction at 10 vol% and 50 vol% as shown in Figure 4.5. Notice that the cut off size of oil droplets is 0.5 μm. The DSD shown in Figure 4.6 also underwent similar way as VMD; the distribution of the droplet was statistical constant.

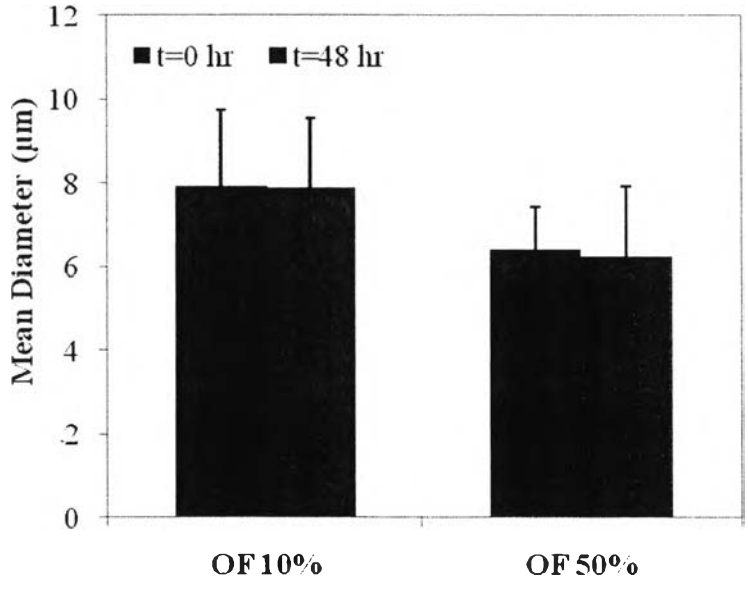

Figure 4.5 Volume-based mean droplets diameter for oil fraction at 10 vol% and 50 vol% over 48 hours.

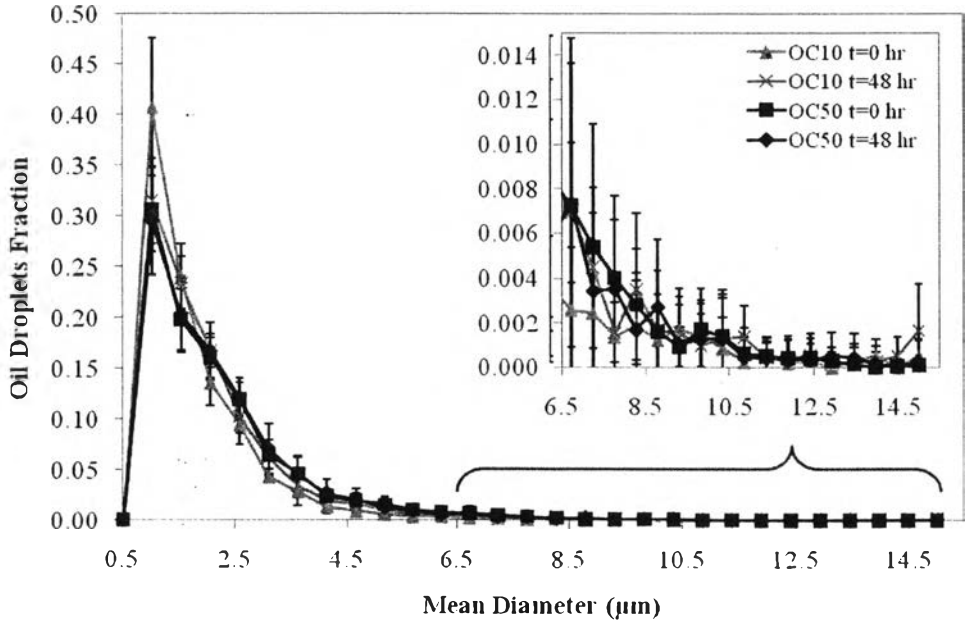

Figure 4.6 Droplet size distribution of oil-in-water emulsion with oil fraction at 10 vol% and 50 vol% over 48 hours.

These analyses revealed that the prepared oil-in-water emulsion was sufficiently stable for conducting further wax deposition experiments.

4.2 Wax Properties and Carbon Number Distribution

The wax used in this study has carbon number distribution of studied wax as shown in Figure 4.7. The carbon number distribution is used as a preference for comparing with the deposit formed from waxy model oil-in-water emulsion.

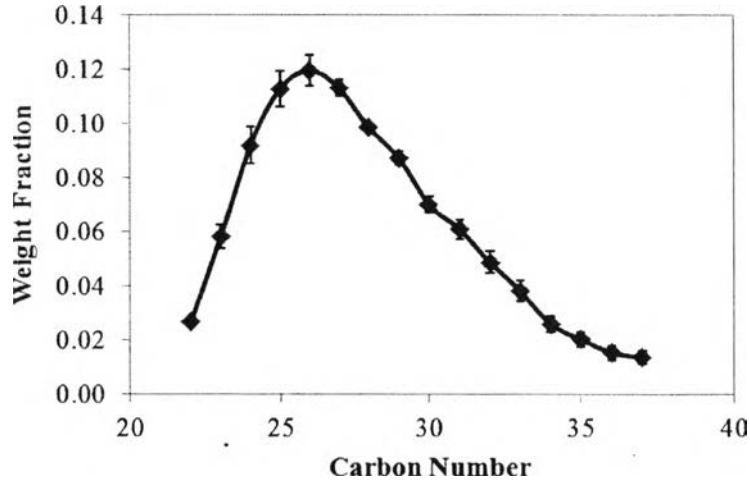

Figure 4.7 Carbon number distribution of studied wax.

4.3 Cold Finger Wax Deposition Experiments

Wax deposition experiments were conducted with cold finger and oil reservoir temperature of 5°C and 45°C, respectively. Deposition characteristics on a clean cold finger surface were first investigated with an emulsion of 50 vol% oil and oil-in-water mixture in absence of surfactant. As shown in Figure 4.8(a), the deposit formed from oil-in-water dispersion could not firmly attach to the deposit surface and tend to slip off the cold finger while the deposit formed by oil-in-water mixture generated a firm attachment of the deposit on the clean cold finger surface shown in Figure 4.8(b). The first speculation according to the deposit formation from oil-in-

water mixture was that clean cold finger surface possibly allowed oil containing wax to get into contact and generated a firmly attaching deposit. On the other hand, the surface properties of cold finger could be changed due to the presence of surfactant. Its surface potentially changed from oil-wetted to water-wetted. Therefore, the deposit could not firmly attach to the clean surface on the cold finger. However, further surface characterization is necessary for explaining the wettability property of clean cold finger.

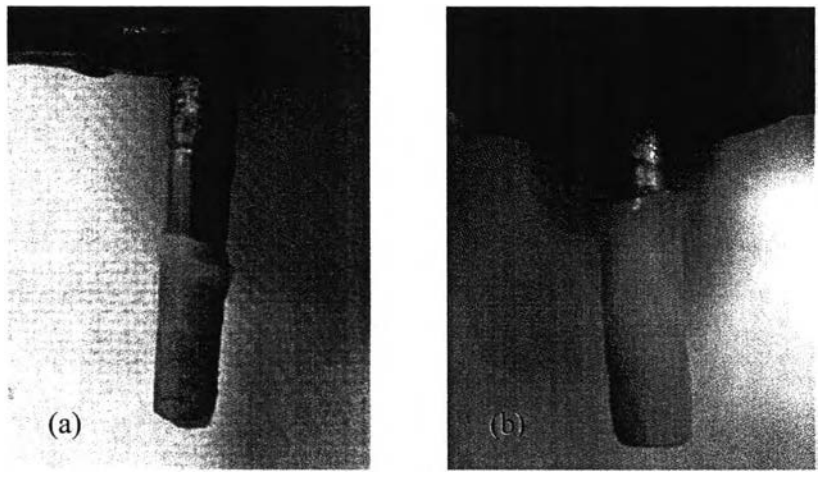

Figure 4.8 (a) Slipped down wax deposit formed from oil-in-water dispersion with oil fraction at 50 vol% on clean cold finger surface, (b) Firmly attaching wax deposit generated by oil-in-water mixture with 50 vol% of oil on un-coated cold finger.

Regardless of surface characterization of stainless steel cold finger, Kumar *et al.* (2011) investigated the interaction force between dispersed oil and steel substrate in water, which was quite similar to our system. They revealed that the formation of oil capillary junction due to the monolayer formation of oil insoluble surfactant. For a short interacting time, the strong repulsive force between the oil and the steel substrate was replaced by attraction force. As interacting time was increased, a large amount of surfactant diffused through water medium, and was adsorbed by the substrate as bilayer resulting in a long repulsion. The bilayer formed from excess diffusing molecules would possibly create a hydrophilic surface which

traps a water layer between this surface and the hydrophilic tails of the surfactant molecules projecting out of the oil droplets. Thus the repulsion is restored.

Based on an observation in Figure 4.8, the sloughing of the deposit from oil-in-water emulsion might undergo previous mechanism, as firmly attached deposit could not be formed on bare stainless steel surface of the cold finger. The surfactant adsorbed on cold finger surface would possibly form a bilayer repelling the dispersed waxy oil droplets in water.

In order to verify the previous speculation, new experiments were proposed using n-C_{28} to pre-coat on the clean cold finger surface prior to continuously generate a wax deposit on the cold finger. With this new proposed procedure, the change in wettability of cold finger might be minimized due to the similarity between coating species and dissolved wax in the reservoir. As indicated by Figure 4.9(a), n-C_{28} can firmly attach to the clean cold finger surface. The reproducible weight of pre-coated element is approximately 0.4814 g which contains wax 14.781 wt% of deposit. Then, the pre-coated cold finger was used to generate a deposit with oil-in-water dispersion. The result shown in Figure 4.9(b), the distinguishable newly formed deposit indicates below the red solid line as an observable thicker layer is generated on pre-coated cold finger surface. From the visual observation, the new proposed possibly allows a subsequent generation of wax deposition onto the n-C_{28} coating element. The deposition characterization was then performed using gas chromatography for analytical affirmation of previous optical observation.

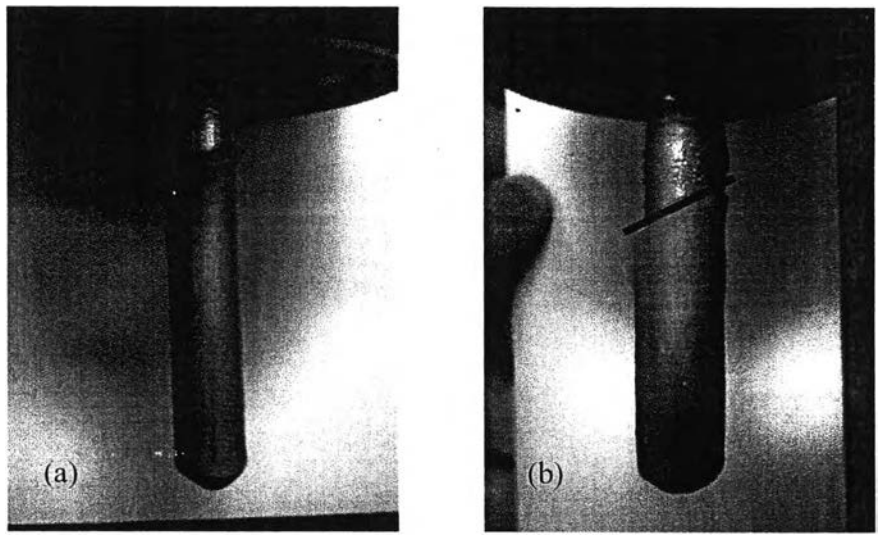

Figure 4.9 (a) Pre-coated cold finger by n-C_{28} coating solution, (b) Newly formed wax deposit generated by oil-in-water emulsion with oil fraction at 50 vol% which can be clearly distinguished from pre-coated surface (below red line).

Gas chromatography was used to characterize both pre-coated n-C_{28} deposit and the newly formed deposit including pre-coated n-C_{28}. Indicating the difference in mole fraction at each carbon number components, the deposit compositions regarding various lengths of n-alkanes were showed in Figure 4.10. The major peak of n-C_{28} was observed owing to a large portion of coating, besides other paraffin components were also observed due to the additional wax. The change in composition of wax deposit confirms a formation of new deposit of dissolved wax in oil-in-water emulsion onto pre-coated n-C_{28} surface.

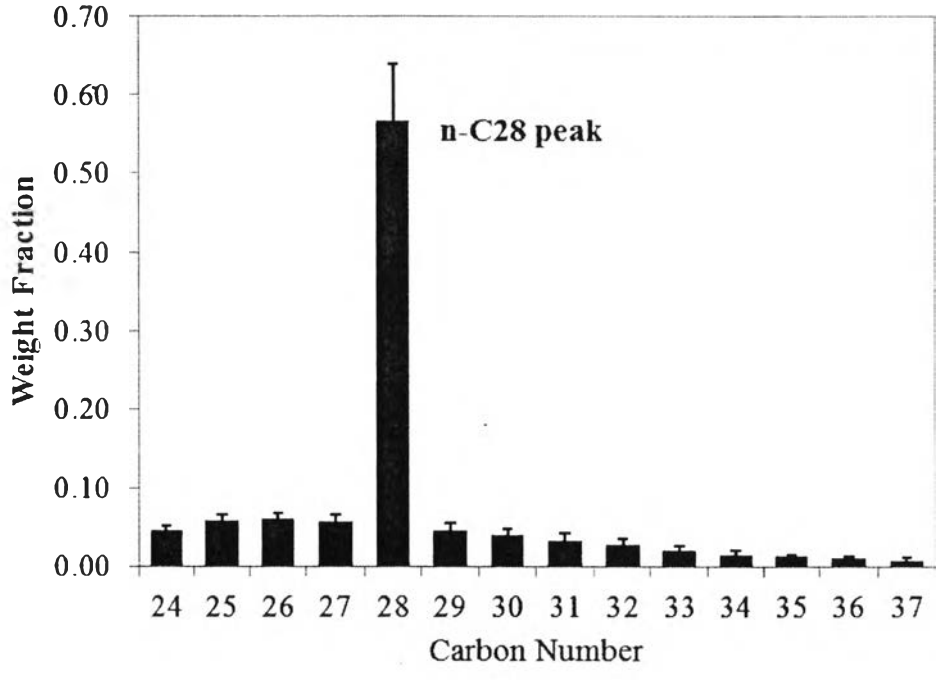

Figure 4.10 Composition distribution of newly formed wax deposit consisting n-C_{28} major peak and other paraffin component peaks.

4.4 Wax Deposition Growth and Wax Content of the Deposit

Wax deposition experiments were performed with two different oil fractions, 5 vol% and 50 vol%. These two experiments were conducted at the same reservoir and cold finger temperature of 45°C and 5°C in order to investigate the role of oil fractions towards wax deposition growth and also wax content of the newly formed deposit from oil-in-water emulsion.

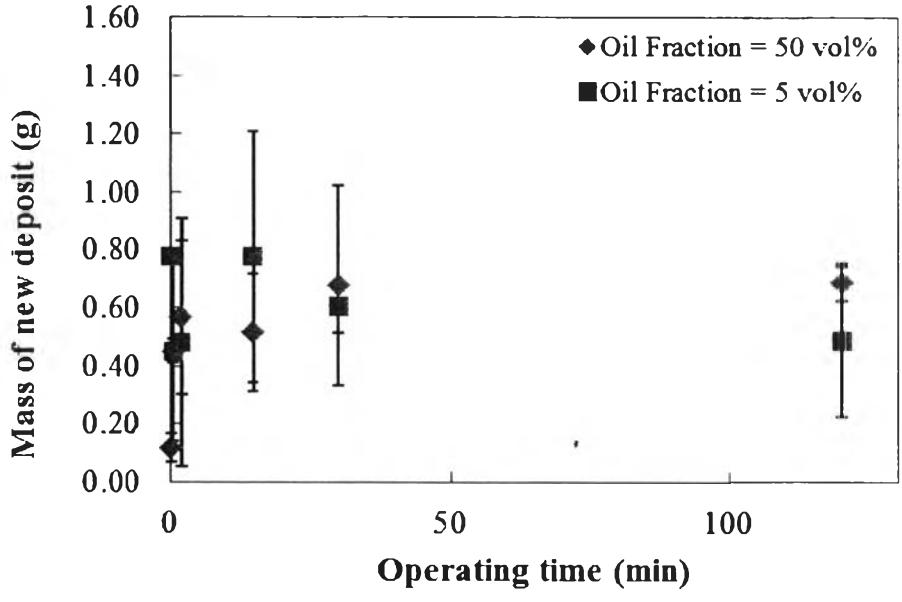

Figure 4.11 Wax deposition growth in short period from oil-in-water dispersion with oil fraction at 5 and 50 vol%.

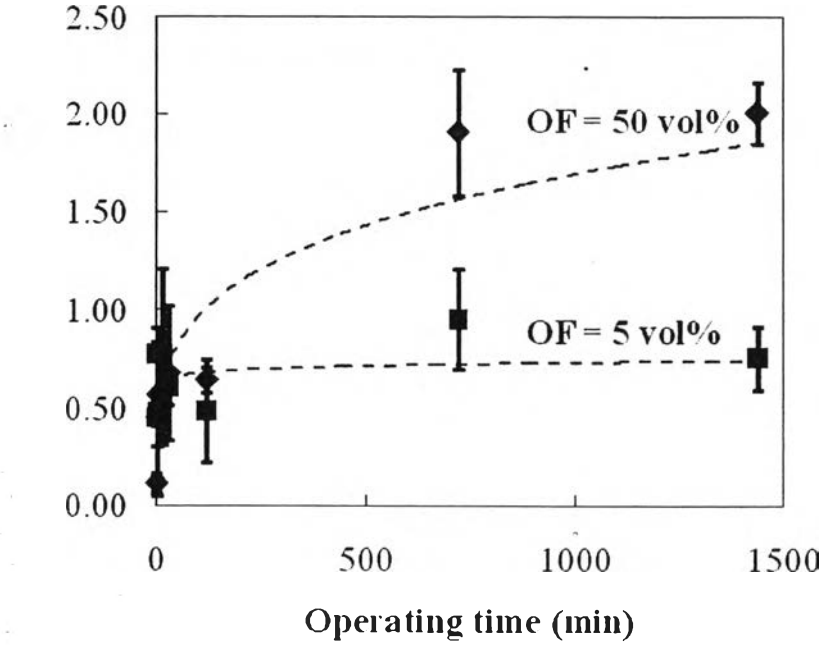

Figure 4.12 The growth rate of wax deposit from oil-in-water dispersion with oil fraction at 5 and 50 vol%.

Figure 4.11 shows the wax deposit mass varied with operating time from 10 seconds to 2 hours for both OF 5 and 50 vol%. As wax deposit growth for both oil fractions reaches plateau rapidly around 2 minutes then remains statistically constant over 2 hours, an error bars are overlapping. Based on short operating time, there is no tendency of wax deposit growing. Therefore, longer operating time experiments were performed and found that the deposit rate with oil fraction at 50 vol% still continue to grow after 2 hours as shown in Figure 4.12. Meanwhile, the deposition growth rate of wax from lower oil fraction remains statistical constant over 24 hours.

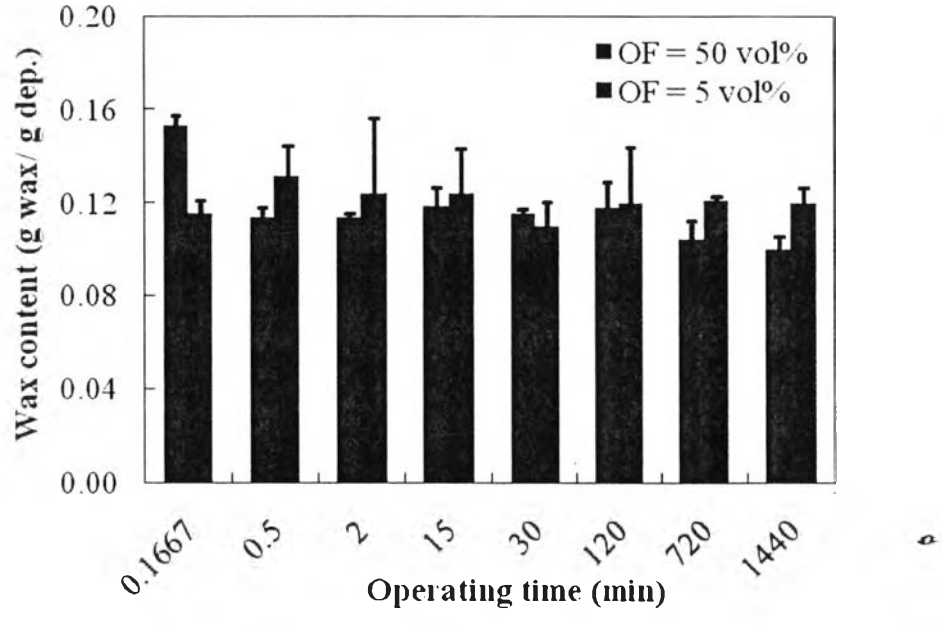

Figure 4.13 Wax content of deposit consisting newly formed deposit and pre-coated C_{28}.

Wax content of the entire deposit including n-C_{28} coating element was analyzed using gas chromatography and found insignificant change with operating time and oil volume fractions. In addition to 10 wt% of added wax in oil continuous phase, n-C_{28} coating element also took into account with wax content; therefore, the wax content values were larger than 10 wt% averagely as shown in Figure 4.13.